

# Ferroelectric Phase Shifters for VHF and UHF\*

M. COHN†, SENIOR MEMBER, IRE AND A. F. EIKENBERG†, MEMBER, IRE

**Summary**—The analysis, construction, and performance of compact surface wave ferroelectric phase shifters suitable for operation in the 100- to 1000-Mc frequency range are described. Although this ferroelectric loaded parallel-plane structure is a very low impedance structure, a satisfactory terminal impedance matching technique has been devised. Kilovolt level voltages are needed; but since the current required to maintain or rapidly shift phase is low, the overall control power requirements are at least an order of magnitude less than those for comparable ferrite phase shifters. One of these room temperature operable phase shifters provided  $348^\circ$  of phase shift at 207 Mc. It had an insertion loss which varied from 3.7 to 2.2 db over a zero- to 4000-volt range of applied dc control voltage.

## INTRODUCTION AND BACKGROUND

**A** THEORETICAL and experimental investigation has been conducted to determine the properties of a surface wave ferroelectric phase shifter operating in the UHF region. In the present application, the term ferroelectric is a misnomer; the property of interest is the nonlinear behavior of the material's dielectric constant in the vicinity of its Curie temperature. The phase-shifting capability results from the fact that the dielectric constant of a ferroelectric material is a function of the magnitude of an applied electric field. The dielectric constant is a function of the applied electric field in a temperature interval extending above the Curie temperature, where the material is not ferroelectric, as well as below the Curie temperature where it is.

The analysis which follows shows that ferroelectric phase shifters are the dual of ferrite phase shifters in many of their characteristics. It will be shown by analysis and measurement, that in the VHF and UHF bands, but not in the higher microwave regions, electric field controlled ferroelectric phase shifters have a number of advantages over their magnetic field controlled ferrite counterparts. These advantages are

- 1) smaller and lighter structures;
- 2) less power required to hold these ferroelectric phase shifters at any arbitrary phase;
- 3) driver energy required to shift phase goes primarily to change the stored electrostatic energy and is not dissipated in the ferroelectric material;
- 4) faster phase shifting;
- 5) the temperature sensitivity is comparable to or better than that of ferrite phase shifters at VHF and UHF;
- 6) possible high power handling capability.

\* Received July 20, 1962; revised manuscript received August 13, 1962.

† Research Division, Electronic Communications, Inc., Timonium, Md.

In order to construct useful devices, a ferroelectric material is needed which does not have excessive losses and which is capable of having its dielectric constant varied over a large range. In addition to the above material requirements, a suitable structure in which to mount the ferroelectric material is needed. Such a structure must permit the signal, which is to be controlled, to be efficiently coupled in and out. It should add a minimum of loss to the irreducible amount determined by the properties of the ferroelectric material. Convenient terminals for the application of the controlling electric field should be available. The geometry should be such that the controlling electric field is applied equally to all or nearly all of the ferroelectric material. A structure which satisfies the above requirements is the partially dielectric loaded parallel-plane waveguide. A cut-away view of the ferroelectric phase shifter built in this waveguide is shown in Fig. 1(a).

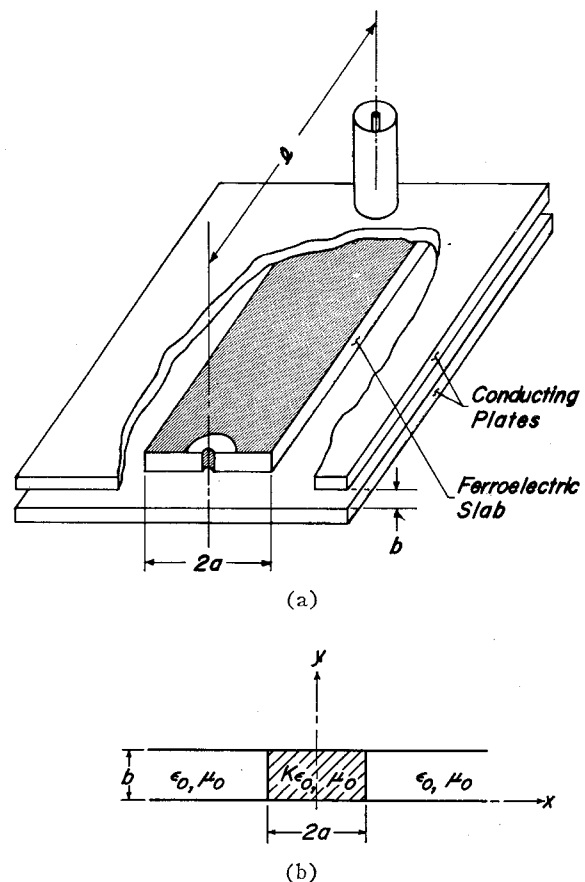


Fig. 1—(a) Cutaway view of the ferroelectric loaded parallel-plane phase shifter. (b) Cross-sectional view of the partially dielectric loaded parallel plane transmission line.

THE PARTIALLY DIELECTRIC LOADED PARALLEL-  
PLANE WAVEGUIDE

The partially dielectric loaded parallel-plane waveguide consists of two infinite parallel conducting planes with a dielectric slab of rectangular cross section between the two planes and contacting each of them. A sketch of this surface wave transmission line, showing the coordinate system used in the analysis, is presented in Fig. 1(b). Prior analyses and confirming measurements [1]–[9] have yielded the properties of this structure. These analyses have shown that there are two classes of surface wave modes ( $PE_{mn}$  and  $PM_{mn}$ ) which can propagate on this structure. The designation PE, which stands for parallel electric, refers to the fact that the electric field lines of these modes lie entirely in planes parallel to the dielectric-air interfaces ( $E_x=0$ ). Similarly the designation PM, which stands for parallel magnetic, refers to the fact that the magnetic field lines of these modes lie entirely in planes parallel to the dielectric-air interfaces ( $H_x=0$ ). The index  $m$  gives the rank of the mode and is indicative of the manner in which the fields within the dielectric strip vary as a function of  $x$ . The index  $n$  gives the order of the mode and equals the number of half cycles of sinusoidal variation of the fields in the  $y$ -direction.

These modes are all hybrid modes, with the exception that the  $n=0$  order PE modes are transverse electric modes ( $TE_{m0}$ ). The  $TE_{10}$  mode, which is the one used in this ferroelectric phase shifter investigation, is the dominant mode. Equations for the field components of the  $TE_{10}$  mode are given below:

Region 1 ( $-a \leq x \leq a$ )

$$E_{y1} = -E_0 \frac{\omega\mu_0}{k_d} \cos k_d x e^{j(\omega t - \beta z)} \quad (1)$$

$$H_{x1} = E_0 \frac{\beta}{k_d} \cos k_d x e^{j(\omega t - \beta z)} \quad (2)$$

$$H_{z1} = jE_0 \sin k_d x e^{j(\omega t - \beta z)} \quad (3)$$

Region 2 ( $x \leq -a$ )

$$E_{y2} = -E_0 \frac{\omega\mu_0}{k_d} \cos k_d a e^{k_2(a+x)} e^{j(\omega t - \beta z)} \quad (4)$$

$$H_{x2} = E_0 \frac{\beta}{k_d} \cos k_d a e^{k_2(a+x)} e^{j(\omega t - \beta z)} \quad (5)$$

$$H_{z2} = -jE_0 \sin k_d a e^{k_2(a+x)} e^{j(\omega t - \beta z)}. \quad (6)$$

Region 3 ( $x \geq a$ )

The field components in region 3 are the same as those in region 2 except that  $e^{k_2(a+x)}$  is replaced by  $e^{k_2(a-x)}$  and the sign of  $H_z$  is changed.

The  $x$ -direction distribution parameters for the dielectric region ( $k_d a$ ) and the outer regions ( $k_2 a$ ) are related by the following equation:

$$k_2 a = k_d a \tan k_d a. \quad (7)$$

The inner or dielectric region  $x$ -direction distribution parameter is related to the wavelength  $\lambda_0$  and the dielectric constant ( $K$ ) and width ( $2a$ ) of the central dielectric slab by the following conditional equation:

$$\pi^2 \left( \frac{2a}{\lambda_0} \right)^2 (K - 1) = \left( \frac{k_d a}{\cos k_d a} \right)^2. \quad (8)$$

For the  $TE_{10}$  mode ( $k_d a$ ) is constrained to be within the interval,  $0 \leq k_d a \leq \pi/2$ . Curves of the  $x$ -direction distribution parameter for the inner region ( $k_d a$ ) and outer regions ( $k_2 a$ ) are respectively shown in Figs. 2 and 3.

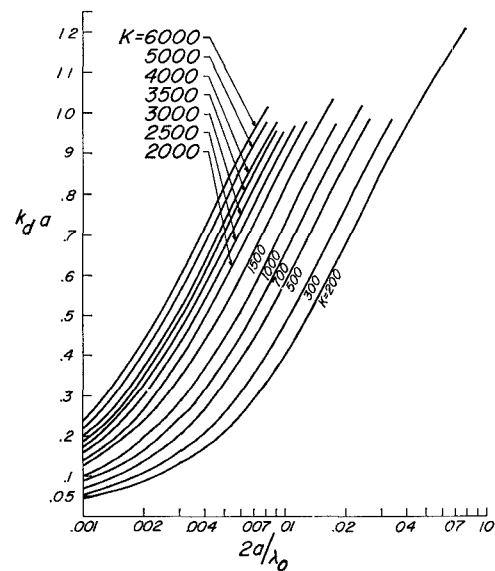


Fig. 2—Curves of the  $x$ -direction distribution parameter for the dielectric region ( $k_d a$ ).

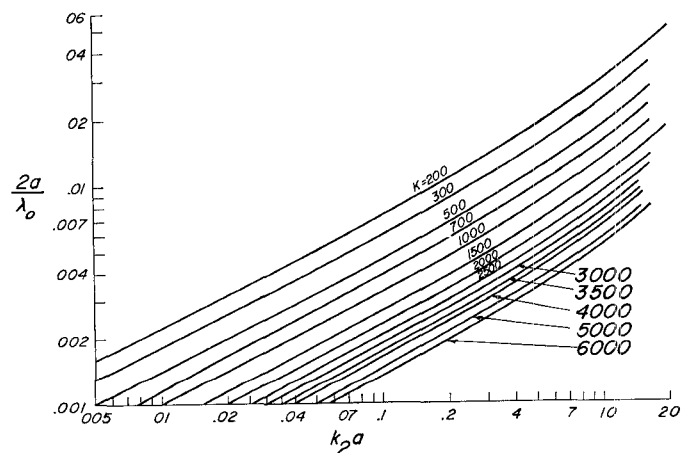


Fig. 3—Curves of the  $x$ -direction distribution parameter for the outer regions ( $k_2 a$ ).

Since the field distribution of the TE modes is not a function of  $y$ , the guide wavelength, cutoff wavelength, and field extent of these modes are independent of the distance " $b$ " between the two conducting planes. This distance can be varied to suppress the hybrid modes, which are a function of  $y$ , and yet not cause the TE modes to be cut off. Curves of the normalized cutoff spacing between the parallel walls ( $b_c/\lambda_0$ ), which assures the fact that all of the hybrid modes ( $PE_{mn}$  and  $PM_{mn}$ ) will be suppressed, are given in Fig. 4. It has been previously shown that for the  $TE_{m0}$  mode to propagate, the following inequality must be satisfied:

$$\frac{2a}{\lambda_0} > \frac{m-1}{2\sqrt{K-1}} \quad (9)$$

The above inequality shows that for the  $TE_{10}$  mode ( $m=1$ ), there is no minimum slab width requirement to be satisfied. Since this mode requires neither a minimum slab width ( $2a/\lambda_0$ ) nor a minimum conducting plane spacing ( $b_c$ ), it can exist down to zero frequency. This mode like the TEM wave on a coaxial line or strip transmission line is thus inherently capable of being used over an extremely broad band of frequencies.

A method of efficiently launching and collecting the  $TE_{10}$  surface wave mode will later be described. That method excites only those TE modes which are symmetric about the  $x=0$  plane ( $m=1, 3, 5$ , etc.). As a result the slab width ( $2a$ ) need only satisfy the following inequality which prevents the  $TE_{30}$  mode from propagating:

$$\frac{2a}{\lambda_0} < \frac{1}{\sqrt{K-1}} \quad (10)$$

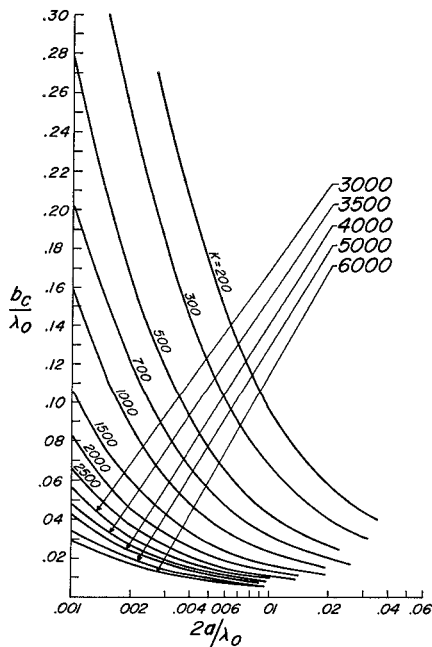


Fig. 4—Curves of the normalized cutoff spacing between the parallel walls ( $b_c/\lambda_0$ ) for suppression of the hybrid modes.

#### PROPERTIES OF THE FERROELECTRIC MATERIALS

A ferroelectric material consisting of a ceramic mixture of 35 per cent lead titanate and 65 per cent strontium titanate was purchased from Gulton Industries, Inc. of Metuchen, N.J. This mixture is referred to in mole per cent. The above material was selected on the basis of having the best room-temperature ratio of voltage tunability to dielectric loss tangent from among a number of materials investigated at the University of Michigan [10].

The material properties were determined from measurements made on small circular parallel-plate capacitors fabricated from the same bars of the ferroelectric material as were used to fabricate the phase shifter slabs. The procedure for fabricating these capacitors and applying gold electrodes to the circular faces is identical to that used in fabricating the larger phase-shifter slabs. This procedure will be described in a subsequent section. The small ferroelectric capacitor (diameter=0.033 inch, height=0.050 inch) was located between the end of the center conductor and an end plate of a special coaxial holder. A thermocouple was mounted on the coaxial holder to monitor temperature. The entire assembly was surrounded by a heating coil. Dc voltages up to 3600 volts can be applied to the ferroelectric capacitor. The diameter of the ferroelectric capacitor was less than the diameter of the inner conductor of the coaxial line and thus uniform dc electric fields can be applied to the capacitor.

The dielectric constant ( $K$ ) and dielectric loss tangent ( $\phi_d$ ) of this material were measured as a function of the applied dc electric field and temperature at a frequency of 200 Mc. These electrical properties were determined from standard input impedance measurements made with a slotted line. The results of these measurements are shown as a function of the applied dc field in Fig. 5. The  $K$  vs  $E$  curves are believed to be quite accurate since these readings depend primarily on the location of the VSWR minimum produced by the ferroelectric capacitor. Since the VSWRs were very high, the minimums were located very accurately. The  $\phi_d$  vs  $E$  curve is considerably less accurate since the values of  $\phi_d$  depend primarily on the magnitude of the VSWR relative to the magnitude of the VSWR produced by a short circuit. The short circuit consists of a copper cylinder, whose dimensions are the same as those of the ferroelectric capacitors. The very high VSWRs were measured by the width of the minimum method. A Starrett dial gauge, accurate to 0.01 mm, was used to determine the width of the minimum. Since the VSWRs due to the ferroelectric capacitor were only slightly less than that due to the short circuit, a small error in the VSWR measurement could result in a large error in  $\phi_d$ .

It should be noted that in the above measurements the ferroelectric element was treated as a lumped capacitor at the end of the coaxial line. If either a sub-

stantially higher frequency or a larger radius ferroelectric capacitor had been used, it would have been necessary to treat the ferroelectric element as a radial transmission line. The conditions of the above reported measurements, however, were such that a negligible error was introduced by the lumped constant treatment.

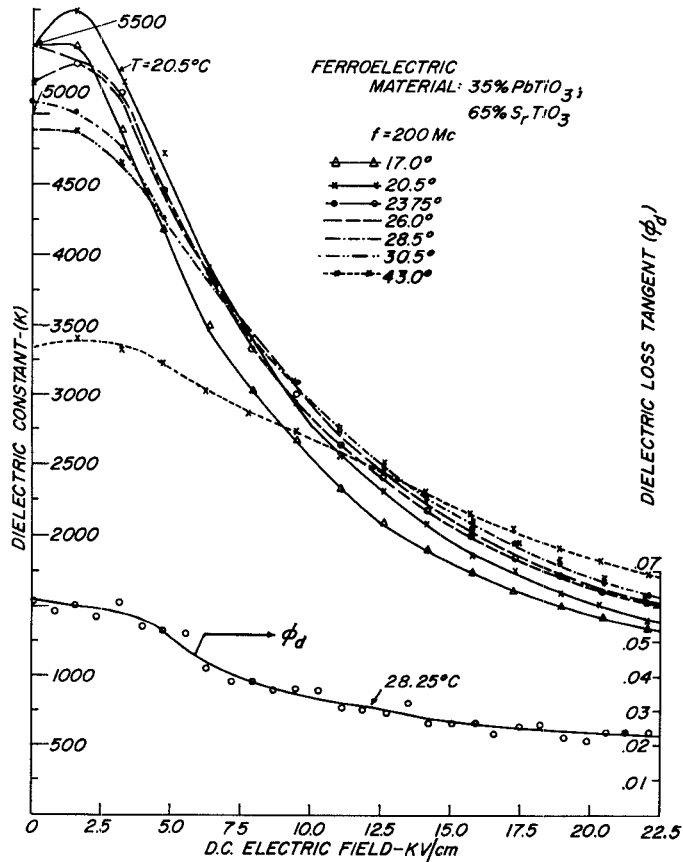


Fig. 5—Measured dielectric constant and loss tangent as a function of applied dc electric field for a ceramic mixture of 35 per cent  $\text{PbTiO}_3$ , 65 per cent  $\text{SrTiO}_3$ .

#### ANALYSIS OF THE FERROELECTRIC PHASE SHIFTER

##### Phase Shifting Properties

It is apparent that the geometric configuration of this surface wave guiding structure lends itself to the development of electric field controlled devices. In the case of the  $\text{TE}_{10}$  mode, the electric field of the controlled RF wave will be parallel to the controlling dc or low-frequency electric field. It has been shown by Diamond [11] that the parallel electric field alignment results in the greatest tunability.

The following analysis of the phase-shifting properties of this structure is an extension of prior analyses [1], [8] of the  $\text{TE}_{10}$  mode performed for linear dielectric materials.

$$\Delta\phi = \Delta(\beta l) = l\Delta\beta, \quad (11)$$

where

$\Delta\phi$  is the incremental change in phase,

$\beta$  is the phase constant of the propagating wave, and

$l$  is the length of the transmission line.

$$\Delta\phi = l \frac{d\beta}{dK} \Delta K + \text{higher order terms}, \quad (12)$$

where  $K$  is the dielectric constant of the ferroelectric material. The higher order terms are neglected in the remainder of this approximate analysis. It has been previously shown [1], [8] that

$$\beta = \frac{1}{a} \sqrt{\pi^2 \left(\frac{2a}{\lambda_0}\right)^2 K - (k_a a)^2}, \quad (13)$$

where  $(k_a a)$  is related to the wavelength ( $\lambda_0$ ), and the width ( $2a$ ) and dielectric constant ( $K$ ) of the ferroelectric slab by (8).

$$\frac{d\beta}{dK} = \frac{\partial\beta}{\partial K} + \frac{\partial\beta}{\partial(k_a a)} \frac{\partial(k_a a)}{\partial K}. \quad (14)$$

From (8), (13) and (14); the following equation for the incremental phase shift is obtained:

$$\Delta\phi = \frac{\pi^2 (l/\lambda_0) (2a/\lambda_0)}{\sqrt{\pi^2 (2a/\lambda_0)^2 K - (k_a a)^2}} \cdot \left[ 1 - \frac{\cos^2 k_a a}{1 + (k_a a) \tan k_a a} \right] \Delta K. \quad (15)$$

A family of curves of the normalized incremental phase shift  $\Delta\phi/(l/\lambda_0)\Delta K$  as a function of the normalized slab width  $(2a/\lambda_0)$  and dielectric constant are shown in Fig. 6. These curves, in conjunction with curves of the dielectric constant as a function of applied dc electric field, enable one to predict the phase shift as a function of the applied field.

##### Dissipative Losses of the Phase Shifter

The RF wave propagating through the phase shifter will be attenuated due to dielectric losses in the ferroelectric material and losses in the two parallel walls of finite conductivity.

The attenuation of the  $\text{TE}_{10}$  mode due to the dielectric loss ( $\alpha_d$ ) has been shown [1], [8] to be given by the following expression:

$$\alpha_d l = \frac{\pi^2 K \phi_d (l/\lambda_0) (2a/\lambda_0)}{\sqrt{\pi^2 (2a/\lambda_0)^2 K - (k_a a)^2}} \cdot \left[ \frac{(k_a a) + \sin k_a a \cos k_a a}{(k_a a) + \cot k_a a} \right], \quad (16)$$

where  $\phi_d$  is the dielectric loss tangent.

A family of curves of the normalized attenuation due to dielectric losses is presented in Fig. 7.

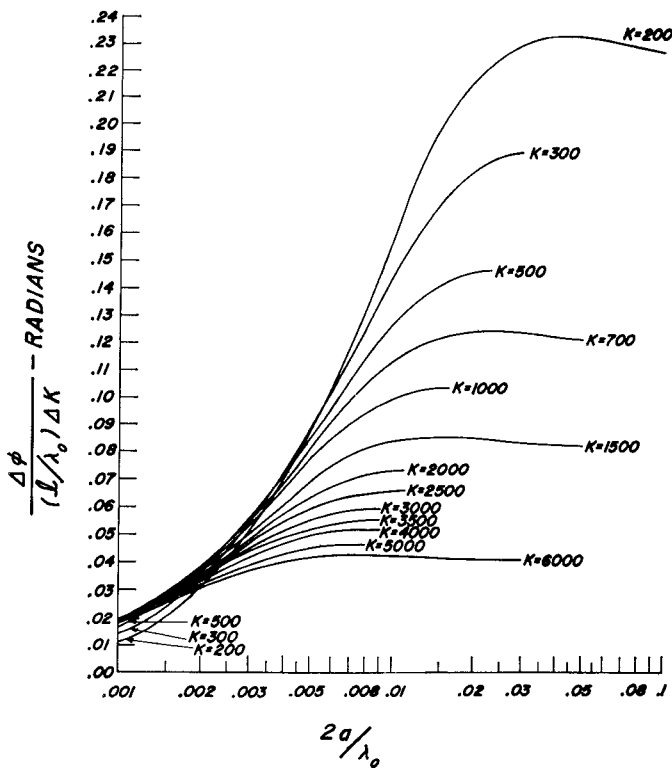


Fig. 6—Normalized phase shift of the ferroelectric loaded parallel-plane waveguide.

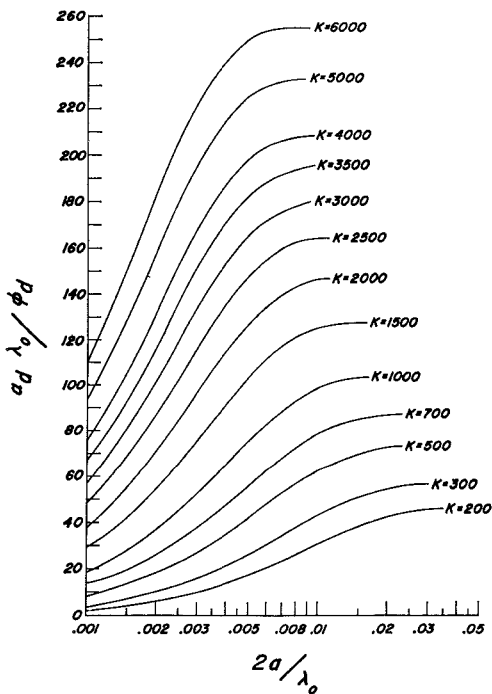


Fig. 7—Attenuation (in nepers per meter) of the TE<sub>10</sub> mode of the dielectric loaded parallel-plane waveguide due to the dielectric loss.

The attenuation due to losses in the parallel conducting walls ( $\alpha_w$ ) has been shown [1], [8] to be given by the following equation:

$$\alpha_w b \sqrt{\lambda_0} = \frac{0.291}{\sqrt{\sigma_w}} \cdot \frac{\left[ \pi^2 \left( \frac{2a}{\lambda_0} \right)^2 K - \frac{(k_{da})^2 \cot k_{da}}{k_{da} + \cot k_{da}} \right]}{\left( \frac{2a}{\lambda_0} \right) \sqrt{\pi^2 \left( \frac{2a}{\lambda_0} \right)^2 K - (k_{da})^2}}, \quad (17)$$

where  $\sigma_w$  is the conductivity of the parallel walls. Curves of the normalized attenuation due to wall losses ( $\alpha_w b \sqrt{\lambda_0}$ ) are shown plotted in Fig. 8. The conductivity of copper ( $\sigma_w = 5.80 \times 10$  mhos per meter) was assumed in computing these curves.

The curves of Figs. 7 and 8, when used in conjunction with curves of the dielectric constant and loss tangent as a function of applied dc electric field, allow one to predict the insertion loss of these phase shifters as a function of the applied field.

A figure of merit ( $M$ ) for this type of phase shifter is the ratio of the phase change produced in a line of length  $l$  to the losses incurred in this length of line.

$$M = \frac{\Delta\phi}{\alpha_d l} \quad (18)$$

Only dielectric losses have been included in the above expression; this is because the few ferroelectric materials which have been investigated at microwave frequencies have relatively high loss tangents, and as a result other sources of loss are negligible in comparison to it. Since

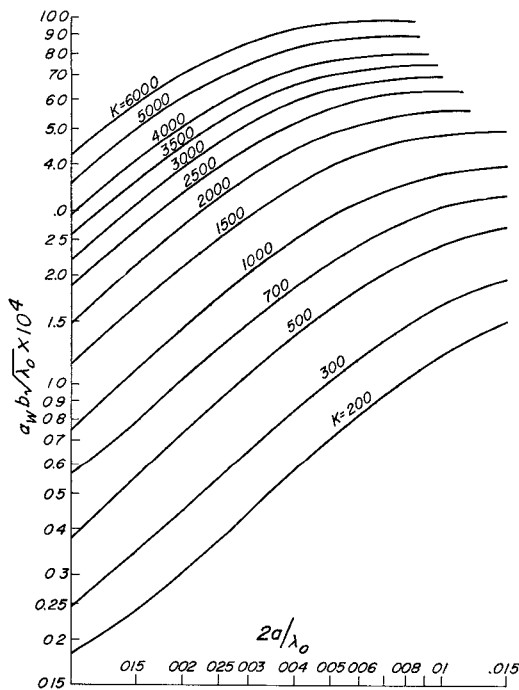


Fig. 8—Attenuation (in nepers per meter) of the TE<sub>10</sub> mode of the dielectric loaded parallel-plane waveguide due to the loss in the parallel conducting walls.

the lengths of line necessary to produce sufficient phase shift are small (even at UHF), it will be shown that the insertion loss of these phase shifters is still reasonable. If ferroelectric materials with sufficiently lower loss tangents are found, then the loss in the parallel conducting planes will be a larger percentage of the smaller total loss and will hence have to be accounted for. Similarly, if in order to reduce the voltage necessary to control the ferroelectric material, the spacing between the parallel planes ( $b$ ) is reduced; then the wall losses increase and they will again have to be accounted for. From (15) and (16), the following equation is obtained:

$$M = \frac{\Delta K}{K\phi_d} \left( \frac{\text{radians}}{\text{neper}} \right) = 6.6 \frac{\Delta K}{K\phi_d} \left( \frac{\text{degrees}}{\text{db}} \right). \quad (19)$$

Eq. (19) indicates the obvious result that the greater the relative change in dielectric constant ( $\Delta K/K$ ) and the less the dielectric loss tangent ( $\phi_d$ ) the better the phase shifter will be. It also shows the non-obvious result, that the figure of merit is independent of the normalized width of the ferroelectric slab ( $2a/\lambda_0$ ). The latter result means that a relatively thick ferroelectric slab can be used with the following advantages:

- 1) The thick slab can be mechanically self-supporting.
- 2) The waveguide wavelength ( $\lambda_g$ ) will be smaller resulting in a shorter section of line being needed to obtain the required phase shift.

The foregoing figure of merit is a useful criterion in selecting ferroelectric materials for this phase-shifter application. A good approximation of the average expected phase-shifter performance in terms of degrees per db can be obtained by using values of  $K$  and  $\phi_d$  for a median value of applied field. It should be noted that in general both  $K$  and  $\phi_d$  are decreasing functions of  $E$ , as shown in Fig. 5. Therefore, if a value of phase shift is prescribed, the insertion loss as deduced from the figure of merit will only be accurate at the median value of applied field. The expected insertion loss will be higher at low fields and lower at high fields.

#### Transverse Field Extent

From (1) through (6) it can be seen that the RF fields in the air spaces of the parallel-plane structure decay exponentially with increasing distance from the dielectric-air interfaces at  $x = \pm a$ . As a result the parallel conducting plates need only extend to a large enough value of  $|x|$  so that these fields have decayed to a sufficiently small value. Experience has shown that it is sufficient if the fields at the plate edges are 20-db down from their value at the dielectric-air interfaces. When the slab width ( $2a$ ), wavelength ( $\lambda_0$ ), and dielectric constant are specified, the curves of Fig. 3 can be used to determine the exponential rate of decay ( $k_2$ ). It is of course neces-

sary to use the lowest value of dielectric constant which is obtained over the range of applied electric field.

An example of this calculation is given below for a phase shifter which was used for many of the measurements to be reported on. The ferroelectric slab consisted of a ceramic mixture of 35 per cent lead titanate and 65 per cent strontium titanate. At a temperature of 20.5°C and a frequency of 200 Mc, the dielectric constant ( $K$ ) varies from 5750 to 1380 within a zero to 22.5 kv/cm range of dc electric field strength (see Fig. 5). The dimensions of the ferroelectric slab are as follows:  $2a = 1.214$  cm,  $b = 0.178$  cm, and  $l = 3.62$  cm.

$$\therefore \frac{2a}{\lambda_0} = \frac{1.214}{150} = .0081$$

From Fig. 3:

for  $K = 1380$

$$k_2 a = 0.61 \text{ nepers}$$

$$\therefore k_2 = \frac{0.61}{0.607}$$

$$= 1.005 \text{ nepers/cm}$$

$$k_2 = 8.72 \text{ db/cm}$$

for  $K = 5750$

$$k_2 a = 1.60 \text{ nepers}$$

$$k_2 = \frac{1.60}{0.607}$$

$$= 2.635 \text{ nepers/cm}$$

$$k_2 = 22.85 \text{ db/cm}$$

The above calculation shows that for the most loosely bound case ( $K = 1380$ ), the conducting plates should be 2.3 cm beyond the edge of the slab for the fields to decay by 20 db from their value at the interfaces. The total width of the conducting plates for this example would thus be 5.814 cm.

It will be shown in a later section that the length of the plates need only be slightly greater than the length of the ferroelectric slab ( $l = 3.62$  cm in this example). These calculations indicate that ferroelectric phase shifters can be very small and hence light in weight even at these low frequencies.

#### Power Requirements to Maintain Constant Phase

Typical values of the dc resistivity ( $\rho$ ) of ceramic mixtures of various titanates lie in the range

$$10^{11} < \rho < 10^{13} \text{ ohm-cm.}$$

Consider the resistance offered to the biasing voltage for a median value of resistivity ( $\rho = 10^{12}$  ohm-cm) and the example of the previous section. The cross-sectional area for bias current flow is

$$A = l \cdot 2a = 3.62 \times 1.214 = 4.40 \text{ cm}^2.$$

$$\therefore R_{dc} = \frac{\rho b}{A} = \frac{10^{12} \times .178}{4.4} = 4.05 \times 10^{10} \text{ ohms.}$$

The dc voltage applied to the phase shifter varies from zero to 4000 volts

$$(I_{dc})_{\max} = \frac{V_{\max}}{R} = \frac{4000}{4.05 \times 10^{10}} = 0.0988 \mu a$$

$$(P_{dc})_{\max} = V_{\max} \times I_{\max} = 4000 \times 0.0988 \times 10^{-6} \\ = 0.396 \text{ mw.}$$

The above calculation shows that the dc power requirements to maintain a fixed phase are extremely small. Therefore the bias power dissipated and hence the heating effects on the characteristics of the ferroelectric material are negligible.

#### Driver Requirements to Shift Phase

The phase shifter as viewed from the terminals of the driving source is essentially a nonlinear parallel-plate capacitor. The capacity vs voltage characteristic of this capacitor will have the same shape as the dielectric constant vs electric field curves shown in Fig. 5. In the previously cited example, the capacitance decreases from 13,580 pf at zero volts to 3700 pf at 4000 volts. It can be shown by an idealized calculation [12], that the energy transferred in changing the voltage from zero to 4000 volts, thereby changing phase by  $360^\circ$ , is about 0.06 joules. The instantaneous current requirements are a function of the speed with which the phase shifting is performed. Although the peak volt-ampere capability of the driver is high, it is at least an order of magnitude less than that required for comparable frequency and speed ferrite phase shifters.

One of the advantages of these phase shifters is that very little of the energy supplied by the driver to effect a rapid change of phase is dissipated in the ferroelectric material or in a portion of the driving circuit which is contiguous to it. The bulk of the energy transferred is used to change the energy stored in the electrostatic field of the capacitor or mechanically stored in the ceramic (these ferroelectric materials are also piezoelectric). Any energy dissipated in the output impedance of the driving circuit should not affect the ferroelectric material since the region of dissipation need not be close by. It is not possible to give a quantitative estimate of the amount of driver power dissipated in the ferroelectric, since a knowledge of the large signal properties of ferroelectric materials would be required. Little information is currently available on the large signal properties of ferroelectrics [13], [14].

#### Temperature Sensitivity

Ferroelectric materials have their greatest voltage tunability ( $\Delta K/\Delta V$ ) near their Curie temperature, and as a result they are most voltage-sensitive in the same temperature range where they are most temperature-sensitive. An estimate of the temperature dependence of

ferroelectric phase shifters can be obtained from the following relationship:

$$\frac{\Delta\phi}{\Delta T} = \frac{\Delta\phi}{\Delta K} \cdot \frac{\Delta K}{\Delta T}. \quad (20)$$

Values of  $\Delta K/\Delta T$  can be determined from curves such as those shown in Fig. 5. At any desired operating point values of  $K(E, T)$  can also be obtained from Fig. 5. This latter information together with the normalized dimensions of the ferroelectric slab,  $(2a/\lambda_0)$  and  $(l/\lambda_0)$  can be used to determine  $\Delta\phi/\Delta K$  from the curves of Fig. 6.

#### Power-Handling Capability

The power-handling capability of these phase shifters would be limited by 1) the RF voltage levels which could be sustained without breakdown, 2) the tolerable temperature rise due to the attenuation of the transmitted RF power, and 3) the material response to large amplitude RF signals.

It has been previously shown [1], [8] that the total power flow ( $P_z$ ) of the  $TE_{10}$  mode of the partially dielectric loaded parallel-plane waveguide is given by

$$\frac{P_z}{abE_{RF}^2} = \frac{4.23 \times 10^{-4}}{(2a/\lambda_0)} \left[ 1 + \frac{\cot k_d a}{k_d a} \right] \\ \cdot \sqrt{\pi^2 \left( \frac{2a}{\lambda_0} \right)^2 K - (k_d a)^2}, \quad (21)$$

where  $P_z$  is the total power flow in watts.

$$E_{RF} = E_0 \frac{\omega\mu_0}{k_d} = \text{amplitude of the RF electric field at } x=0 \text{ in volts per meter.}$$

The above function is shown plotted in Fig. 9. Using the above curves for the worst case of our example ( $K=1500$ ), it is found that  $P_z=37.2$  kw for a peak RF electric field of 2 kv/cm ( $E_{RF}=2 \cdot 10^5$  volts/meter). A larger value for the RF field was not used in the above calculation since it must be superimposed on the dc electric field.

If the width of the ferroelectric slab is sufficiently small, the power-handling capability before voltage breakdown is very high. Reducing the width of the ferroelectric slab increases the length of line necessary to produce a prescribed phase shift. It has been shown, however, that the figure of merit ( $M$ ) and hence the average insertion loss is independent of the slab width. The same quantity of RF power will thereby be dissipated over a greater length of transmission line, thus causing a diminished heating effect on the ferroelectric. The price of this advantage in power-handling capability is that the advantage of small size is partially lost.

It should be noted that since the conducting planes of this structure are in intimate contact with the ferroelectric slab, heat removal by natural or artificial means is facilitated.

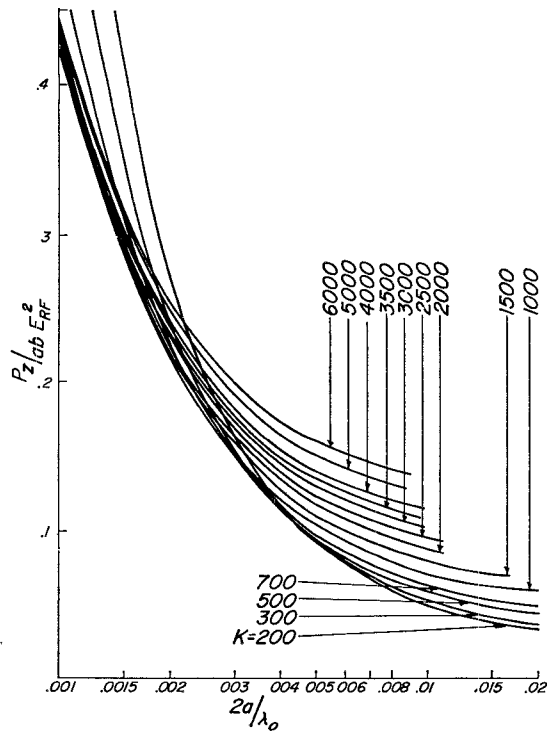


Fig. 9—Power-handling capability of the TE<sub>10</sub> mode.

The effects of large amplitude RF voltages on the properties of ferroelectric materials are largely unknown and would have to be determined by experiment. Although only limited information is available [13], [14], it is likely that large RF fields will cause nonlinear behavior, *e.g.*, harmonic generation, mixing, and electromagnetic shock wave generation.

#### Impedance

A useful value of impedance, which agrees with measured results is obtained from a power-voltage relationship. For a lossless transmission line, this impedance is of course purely resistive. It will be denoted by the symbol  $R$ .

$$R = \frac{[V(x=0)_{\max}]^2}{2P_z} = \frac{E_{RF}^2 b^2}{2P_z}. \quad (22)$$

Through the use of (21), this impedance relationship can be put in the following normalized form:

$$R \left( \frac{a}{b} \right) = \frac{120\pi \cdot \pi(2a/\lambda_0)}{\sqrt{\pi^2(2a/\lambda_0)^2 K - (k_d a)^2 \left(1 + \frac{\cot k_d a}{k_d a}\right)}}. \quad (23)$$

Families of curves computed from (23) are shown in Fig. 10. These curves show that for typical geometric parameters ( $a$  and  $b$ ), the ferroelectric loaded parallel-plane waveguide is a very low impedance transmission line. That is of course an expected result, since the dielectric constants are so high. These low impedance values result in a severe terminal impedance matching

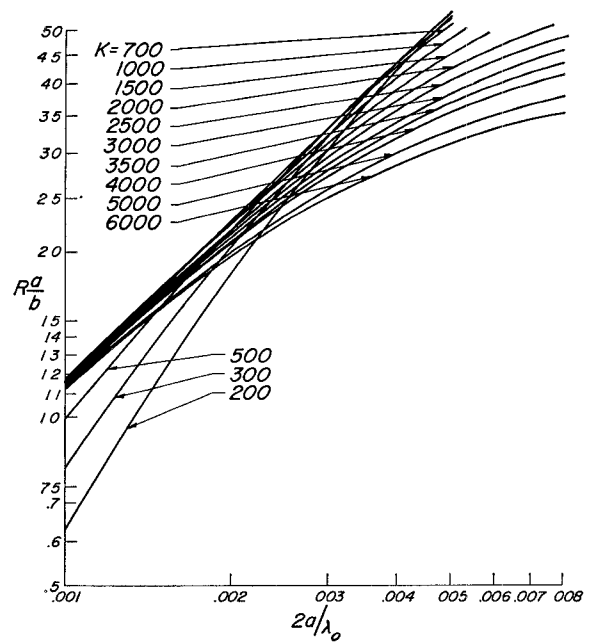


Fig. 10—Normalized impedance  $[R(a/b)]$  of the TE<sub>10</sub> mode.

problem. It will be shown, however, that it is an advantage with regard to the surface wave launching and collecting problem.

#### Excitation of the TE<sub>10</sub> Mode

The method of launching the desired TE<sub>10</sub> mode on this ferroelectric loaded surface wave line consists of using a transverse current filament which is perpendicular to and extends across the space between the parallel conducting walls. It would be centered in the dielectric slab ( $x=0$ ). This current filament can be energized from a coaxial line feeding through one of the conducting planes with only the center conductor crossing the parallel-plane line and contacting the opposite wall (see Fig. 1(a)).

The above launching technique has been previously analyzed [15] and found to be extremely efficient and broad-banded. In particular it was found to be particularly well suited to the launching of this mode on very high dielectric constant materials. The analysis has shown that as long as the dielectric constant is large ( $K > 100$ ), the efficiency with which the TE<sub>10</sub> mode can be launched is nearly independent of the dielectric constant. Changes of the dielectric constant, due to electric field changes, therefore will not affect the launching efficiency.

The above method of launching the TE<sub>10</sub> mode is inherently bidirectional, *i.e.*, equal amounts of surface wave power will be launched in the positive and negative  $z$ -directions. Eq. (23) shows that at abrupt terminations of the ferroelectric slab the ratio of the impedance in the dielectric loaded portion ( $0 < z < l$ ) to that in the unloaded portion ( $z < 0$  and  $z > l$ ) is very small. The abrupt terminations of the ferroelectric slab serve as open circuit walls.



### PREPARATION OF THE FERROELECTRIC SLABS

Prior to assembling and testing the ferroelectric phase shifter, considerable experimentation was performed in order to determine satisfactory methods for fabricating the ferroelectric slabs and applying the required electrodes. Until a satisfactory procedure was evolved, considerable difficulty with high-voltage breakdown was experienced. It was found that the lead titanate-strontium titanate ceramic materials could be satisfactorily machined with diamond cutting wheels, grinding wheels, and drills. After machining the basic slab shape, small half holes were drilled in the ends of the slab (see Fig. 1(a)). These half holes accept the extended center conductors of the coaxial lines which serve as current filament launchers and collectors.

Electrodes were applied to the two longitudinal surfaces of the slab which are perpendicular to the axes of the half holes. The electrodes also covered the walls of the half holes. The diameter of the half holes is 0.015 inch and the outer diameter of the annular regions is 0.125 inch. When inserted in the parallel-plane phase shifter, the upper surface, containing the annular regions is maintained at ground potential. The high-voltage electrode consists of the bottom surface and the walls of the half hole which are in contact with it.

The first electrodes used consisted of Du Pont No. 4731 silver paint. These electrodes were oven-baked onto the ceramic slab for one hour at a temperature of 600°C. It was observed that the insertion loss of phase shifters with these silver electrodes increased with time. There is evidence in the technical literature [16] which indicates that silver tends to migrate through ceramics due to the action of high electric fields and elevated temperatures. It is believed that the silver migration causes increased dielectric losses and decreased dielectric strength of the host ceramic.

As a result of the observed aging effects of silvered ferroelectric slabs, all of the remaining phase shifter slabs fabricated during this investigation had gold electrodes. These electrodes consisted of Du Pont No. 6976 gold paste, which is brushed on and then baked at a temperature of 760°C for about one hour. The resulting coating is very thin, and as a result as many as five successive coats had to be applied to obtain sufficient thickness and avoid holes in the coating. It was found that the gold electrodes, like the silver electrodes, adhered well and had very high conductivity. Over a period of eight months, no aging effects have been observed with the gilded units.

In order to reduce the wall losses due to the thin and granular baked-on gold electrodes, solid gold electrodes were attached to the upper and lower surfaces of the ferroelectric slab. These electrodes were cut from 0.004-inch thick gold sheet stock. Du Pont No. 6976 gold paste was used to attach the gold sheets to the previously gilded ferroelectric surfaces. The resultant unit can be handled with considerably less caution than was previously required. Fear of cracking the slab

or scratching the formerly thin electrodes has been reduced.

An adhesive backed mylar tape (0.001-inch thick) is applied to all ungilded surfaces of the ferroelectric slab (including the half annular regions). The mylar tape helps to prevent high voltage breakdown across these surfaces. Ferroelectric slabs, prepared as described above, have withstood electric field intensities up to 27 kv/cm. A number of thin samples, similarly prepared, have sustained fields up to 160 kv/cm.

### Measured Phase-Shifter Performance

Measurements of phase shift as a function of the dc electric field and temperature were made with a phase-sensitive bridge circuit in which the movable probe of a slotted line served as a null detecting device. The insertion loss was measured by a standard RF substitution technique. Two very small coaxial dc blocks were constructed in order to measure the input and output impedance of the phase shifters as a function of the dc field. These dc blocks were very small in order to make impedance measurements as close as possible to the ends of the ferroelectric slab. The blocking capacitor consisted of a thin circular wafer of ferroelectric material with thin gold electrodes baked on each circular face. The wafer diameter and thickness were 0.340 inch and 0.020 inch respectively. The diameter of the gold electrodes was 0.220 inch. The above ferroelectric capacitor is capable of withstanding a voltage of 4000 volts. The input and output impedance of a phase shifter containing the slab whose transverse dimensions were  $2a=1.214$  cm and  $b=0.178$  cm was measured at 200 Mc. It was found that the terminal impedances were close to purely real and varied from 1.8 ohms at zero dc field to 1.3 ohms at about 20 kv/cm. These measured impedances are in excellent agreement with those determined from Fig. 10.

As a result of the above impedance measurements, Teflon-filled coaxial quarter wave transformers, which provide a 33:1 impedance transformation were connected to each port of the phase shifter. Double stub tuners were used at each end of the assembly. These tuners were adjusted to provide an intrinsic match at each port via the method described by Tomiyasu [17]. Commercial coaxial dc blocks were located between the quarter wave transformers and stub tuners so that the high dc voltage (up to 4000 volts) was constrained to the lower conducting plate and the coaxial center conductors up to the dc blocks.

The lead titanate-strontium titanate ferroelectric slab, used for these measurements, was fabricated to the following dimensions:  $2a=1.214$  cm,  $b=0.178$  cm,  $l=3.62$  cm. This slab was mounted between parallel plates, whose dimensions are 4 inches  $\times$  3 inches  $\times$   $\frac{1}{8}$  inch thick. These plate dimensions are more than ample for the specified slab geometry at frequencies in the vicinity of 200 Mc. The phase shifter was placed in a small phenolic box so that the lower high voltage plate

is not exposed. The phenolic box also serves as a container for the sulfur hexafluoride gas.

A photograph of the assembled ferroelectric phase shifter is shown in Fig. 11. The external matching structure used in the measurements is also shown. The plastic hose attached to the upper plate is used to fill the phase shifter with sulfur hexafluoride gas.

Using the previously described procedure, the phase shift and insertion loss of this phase shifter was measured as a function of dc electric field at a number of temperatures from 17°C to 43°C and at a number of frequencies near 200 Mc. The input and output VSWRs were measured by a conventional slotted-line technique. Prior to making these measurements, the double stub tuners were adjusted to provide an intrinsic match at each port for the following condition:  $f=200$  Mc,  $T=23.75^\circ\text{C}$ ,  $E_{dc}=4.0$  kv/cm. During the remainder of the measurements to be reported, the tuners were not readjusted.

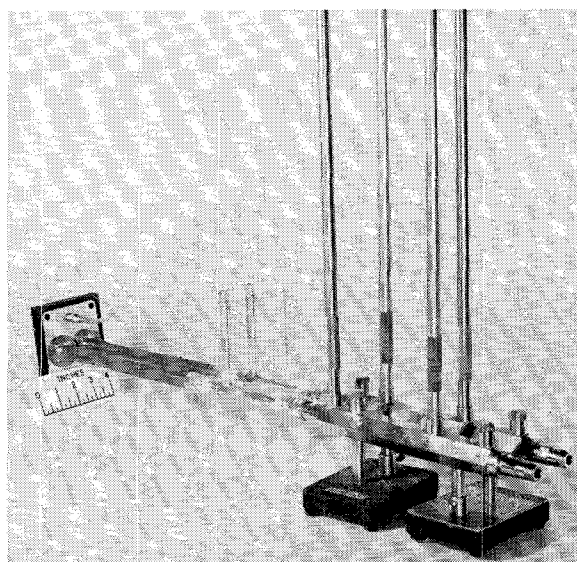


Fig. 11—Photograph of the assembled ferroelectric phase shifter showing the external matching structure.

The results of these measurements at 200 Mc for a number of temperatures are shown in Figs. 12, 13 and 14 (next page). Since the input and output VSWRs are nearly identical, only the input VSWRs are shown. An additional 0.8 db of insertion loss due to the quarter wave transformers, dc blocks and double stub tuners at each port is not included in the insertion loss curves.

Note that except for the  $T=20.5^\circ\text{C}$  case the phase-shift curves do not reach zero degrees. This is because a fixed reference phase was maintained for all temperatures. That in turn was done so that the phase-shift curves at different temperatures could be compared to determine the temperature sensitivity of this phase shifter. Comparing the  $20.5^\circ\text{C}$  and  $23.75^\circ\text{C}$  phase-shift curves it can be seen that the temperature sensitivity within this  $3.25^\circ\text{C}$  temperature interval has the

following values:

| $E_{dc}$<br>(kv/cm) | $\Delta\phi/\Delta T$<br>(degrees phase shift/ $^\circ\text{C}$ temperature change) |
|---------------------|---|
| 0                   | 4.6   |
| 1.25                | 1.5   |
| 2.50                | 4.6   |
| 5.00                | 5.4   |
| 7.50                | 2.2   |
| 10.00               | 0.6   |
| 12.50               | 1.4   |
| 15.00               | 1.4   |
| 17.50               | 1.8   |
| 20.00               | 2.0   |
| 22.50               | 3.1   |

It should be noted that over a larger temperature interval, the temperature sensitivity will be larger. Although the above temperature sensitivity figures are comparable to those of ferrite phase shifters at these low frequencies, they indicate the need for temperature control of these units.

At  $28.5^\circ\text{C}$  the dc current drawn by this phase shifter was measured as a function of the applied electric field. The results are shown on Fig. 14. The very low current ( $I_{dc} < 0.1 \mu\text{a}$ ) corresponds to a dc resistivity of  $1.4 \times 10^{12}$  ohm cm. The maximum dc power dissipated in the ferroelectric slab is 0.28 mw.

Calculated phase shift and insertion loss curves have not been shown on these curves. Some calculations have been made, and they show that the calculated and measured phase shift curves track within a few per cent. The measured and calculated insertion loss curves are in excellent agreement at low dc fields. At high fields the measured loss does not decrease as fast as the calculated loss.

The theoretical curves of  $\Delta\phi$  (Fig. 6) and  $\alpha_d$  (Fig. 7) show that, for the values of  $2a$  and  $\lambda_0$  used in these final measurements, the phase shift and dielectric loss should increase nearly linearly with frequency in much the same manner as a TEM wave ferroelectric phase shifter. If a thinner slab were used (smaller  $2a/\lambda_0$ ), the operating point would not be at a point where the normalized  $\Delta\phi$  and  $\alpha_d$  curves had leveled off. In that case the phase shift and dielectric component of attenuation would increase at a greater than linear rate with frequency. Similarly the theoretical impedance curves (Fig. 10) show that the input and output impedance of the phase shifter should be slowly varying functions of frequency.

The most frequency-sensitive elements used in these measurements were the external impedance matching structures. Nevertheless measurements of phase shift, insertion loss, and input VSWR vs the applied dc electric field were made for a number of frequencies between 196 and 214 Mc at a temperature of  $23.75^\circ\text{C}$ . The best results were obtained at 207 Mc, where a phase shift of  $348^\circ$  was obtained. Insertion loss varied

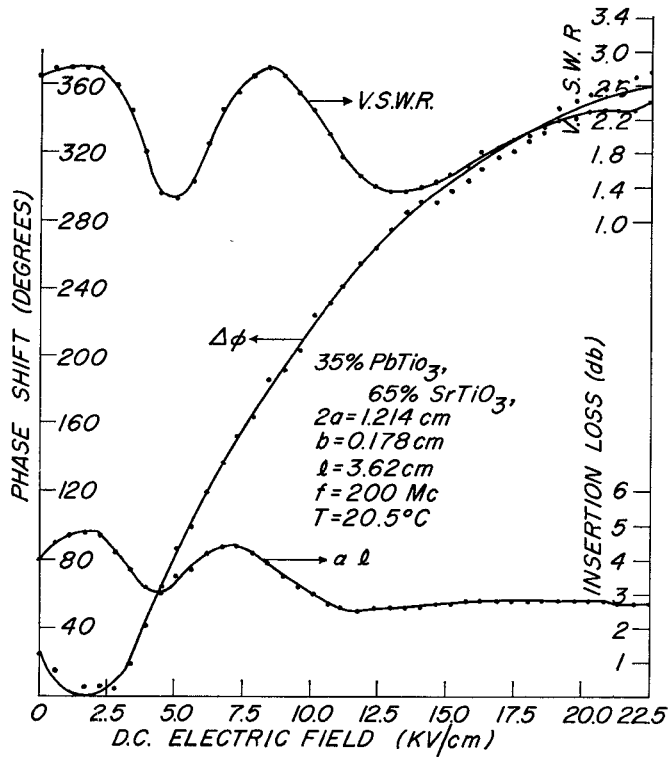


Fig. 12—Measured performance of the ferroelectric phase shifter;  $f=200$  Mc,  $T=20.5^\circ C$ .

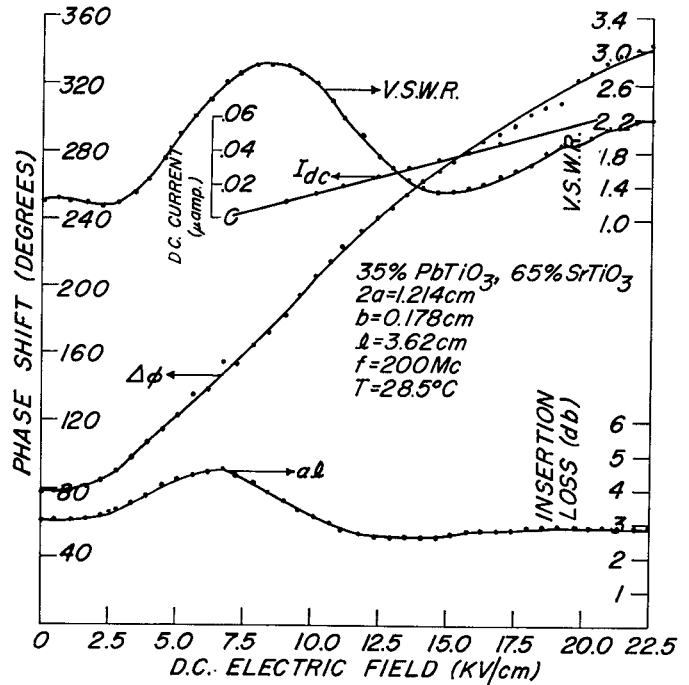


Fig. 14—Measured performance of the ferroelectric phase shifter;  $f=200$  Mc,  $T=28.5^\circ C$ .

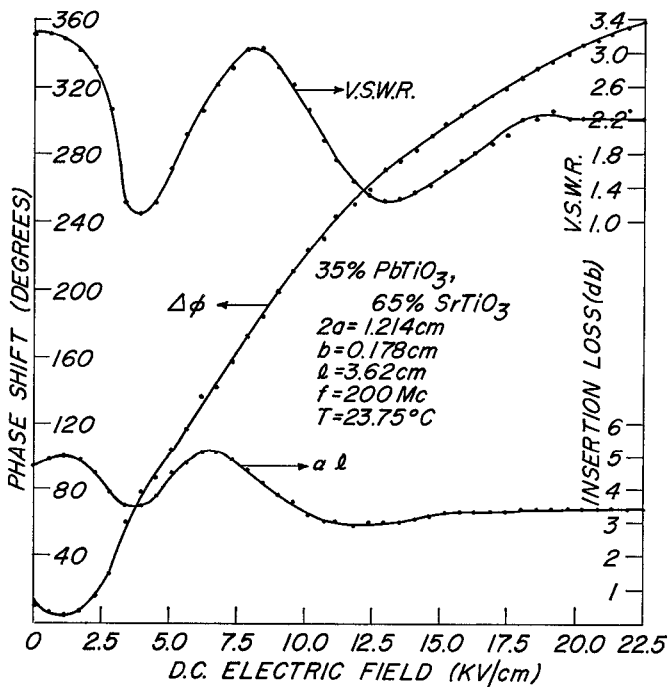


Fig. 13—Measured performance of the ferroelectric phase shifter;  $f=200$  Mc,  $T=23.75^\circ C$ .

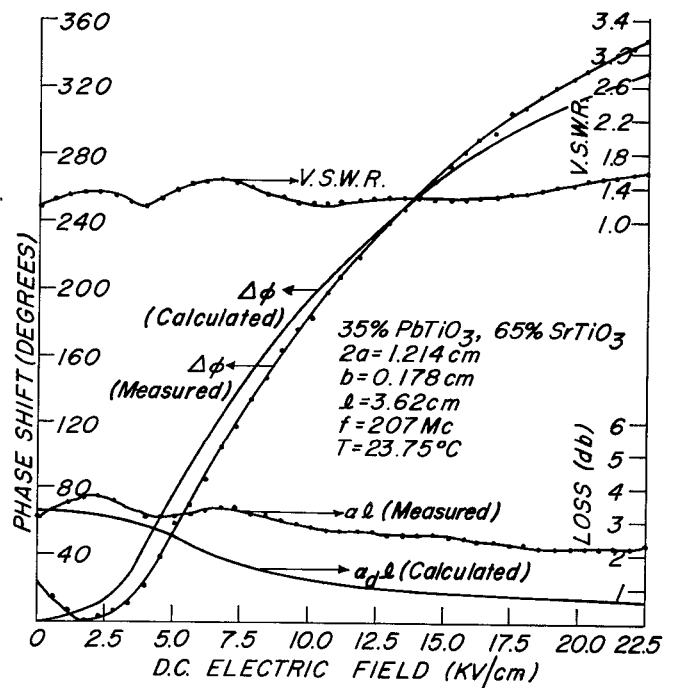


Fig. 15—Measured and calculated performance of the ferroelectric phase shifter;  $f=207$  Mc,  $T=23.75^\circ C$ .

from 3.7 db down to 2.2 db over the range of dc field strength. Input VSWR varied from 1.14 to 1.56.

The 207-Mc data is shown on Fig. 15. For comparison purposes, the theoretically computed curves of phase shift ( $\Delta\phi$ ) and insertion loss due to the dielectric loss ( $\alpha_d l$ ) are also presented. The computed and measured phase-shift curves are in excellent agreement. At low values of the dc electric field, the calculated dielectric losses account for nearly all of the measured loss. Reflection losses and wall losses are a larger percentage of the reduced total loss at high dc fields.

In addition to limiting the bandwidth, the external matching structure is very large. As a result, one of the principal advantages of ferroelectric phase shifters, *e.g.*, their small size, is partially nullified. Impedance measurements made through the previously described small dc blocks, employing ferroelectric discs as blocking capacitors, indicated that each port of the phase shifter could be intrinsically matched with a lumped shunt capacitance. These capacitors would be located in the coaxial feed lines within a few centimeters of the current filament launchers and collectors. A graphical analysis performed on a Smith Chart shows that this method of impedance matching is extremely broadbanded.

#### CONCLUSIONS AND RECOMMENDATIONS

The theoretical analysis of the ferroelectric loaded parallel-plane phase shifter together with some published data on the electrical properties of ferroelectric materials shows that at frequencies below 1000 Mc, useful electric field controlled phase shifters can be developed. Results obtained during this investigation have shown that the measured and predicted phase shifts are in excellent agreement. At low dc fields, where the intrinsic matching is performed, the predicted and measured losses are also in good agreement. At high fields, where the predicted losses decrease, the agreement is poorer because the reflection losses increase and are a larger portion of the total loss. Obtaining a good impedance match to the characteristically low impedance ferroelectric structure is difficult, but feasible.

Although the temperature sensitivity of ferroelectric phase shifters is a problem to be reckoned with, it is not as difficult a problem as is often cited. In the case of the parallel-plane phase shifter, the structure lends itself to temperature control. For high RF power levels, the use of a ferroelectric material having a high Curie temperature may be desirable. For example a ceramic mixture consisting of 45 per cent lead titanate and 55 per cent strontium titanate would have a Curie temperature in the vicinity of 90°C. A phase shifter, using this material and equipped with a heater and thermal switch, could be maintained at the optimum temperature over a large range of ambient temperatures and internal power dissipation levels.

The measured dc current flowing through these phase shifters has verified the predicted low bias power required to maintain any fixed phase. Although rapid phase-shifting measurements were not made, analysis has shown that the driver current and power requirements are at least an order of magnitude less than for comparable ferrite phase shifters. In addition only a small percentage of the driver output is dissipated in or near the ferroelectric phase shifter.

Until a few years ago, ferroelectricity was regarded as a unique property observed in only a few materials. Within the past decade many materials have been found to be ferroelectric, but only a few of these materials have been investigated at frequencies above the audio range. Among those materials tested up to the microwave region, only single-crystal strontium titanate [18], [19] has a substantially lower dielectric loss tangent than the lead titanate-strontium titanate mixture used in this investigation. Pure strontium titanate (ceramic or single crystal), however, must be maintained at temperatures near or lower than that of liquid nitrogen in order to achieve a large voltage tunability. Among the materials with more convenient operating temperatures, there probably are some with a better figure of merit than that of the material used in this investigation.

It should be noted that the achieved phase-shifter performance is such that only a slight figure of merit improvement is needed.

With presently known materials, ferroelectric phase shifters offer their greatest advantages at frequencies less than 1000 Mc. At these frequencies, their high dielectric constants result in compact yet not inconveniently small components. It is also a frequency range where ferrite phase shifters are less suitable because of their large size, large holding and driver-power supply requirements, and sluggish response.

Although the results achieved thus far are encouraging, a great deal of additional development work is needed to produce a satisfactory operational ferroelectric phase shifter. Lower-loss ferroelectric materials would be desirable and for many applications a necessity. It is hoped that the results of this study will provide an incentive for further investigations leading to improved ferroelectric materials.

#### ACKNOWLEDGMENT

The authors would like to thank A. E. Snider and C. W. Hicks for making many of the preliminary measurements and devising some of the fabrication techniques used on the ferroelectric slabs. We would also like to thank Marcia J. King for computing and plotting many of the theoretical curves of this paper. Acknowledgment is also due to M. A. Kott of the Johns Hopkins University Radiation Laboratory for supplying some of the computed results used in Figs. 2, 3, 4, 7, and 8.

## REFERENCES

- [1] M. Cohn, "Propagation in Partially Dielectric Loaded Parallel Plane and Trough Waveguides," The Johns Hopkins University Radiation Laboratory, Tech. Rept. AF-78; July, 1960.
- [2] F. J. Tischer, "Mikrowellenleitung mit geringen Verlusten" (Waveguides with small losses), *Arch. elekt. Übertragung*, vol. 7 pp. 592-596; December, 1953.
- [3] F. J. Tischer, "The H-guide, a waveguide for microwaves," IRE NAT'L CONVENTION RECORD, pt. 5, pp. 44-47; 1956.
- [4] F. J. Tischer, "Properties of the H-guide at microwaves and millimeter waves," IRE WESCON CONVENTION RECORD, pt. 1, pp. 4-12; 1958.
- [5] R. A. Moore and R. E. Beam, "A Duo-dielectric Parallel Plane Waveguide," *Proc. Nat'l Electronics Conf.*, vol. 12, pp. 689-705; April, 1957.
- [6] M. Cohn, "Attenuation of the  $HE_{11}$  mode in the H-guide," IRE TRANS. ON MICROWAVE THEORY AND TECHNIQUES, vol. MTT-7, pp. 478-480; October, 1959.
- [7] J. W. E. Griemsmann and L. Birenbaum, "A Low Loss H-Guide for Millimeter Wavelengths," Microwave Research Inst. Symposia Series, vol. 9, pp. 543-562, New York, N. Y.; 1959.
- [8] M. Cohn, "Propagation in a dielectric-loaded parallel plane waveguide," IRE TRANS. ON MICROWAVE THEORY AND TECHNIQUES, vol. MTT-7, pp. 202-208; April, 1959.
- [9] M. Cohn, "TE modes of the dielectric loaded through line," IRE TRANS. ON MICROWAVE THEORY AND TECHNIQUES vol. MTT-8, pp. 449-454; July, 1960.
- [10] C. B. Sharpe and C. G. Brockus, "Investigation of Microwave Properties of Ferroelectric Materials," The Univ. of Mich., Dept. of Elect. Engr., Electronic Defense Group, Final Rept. on Contract No. DA-36-039sc-75003; March, 1959.
- [11] H. Diamond, "Polarization, Microwave Dispersion, and Loss in High Permittivity Ferroelectrics," Willow Run Labs., The Univ. of Mich., Rept. of Project Michigan on Contract No. DA-36-039sc-78801; January, 1960.
- [12] M. Cohn and A. F. Eikenberg, "UHF Ferroelectric Phase Shifter Research," Electronic Communications, Inc., Final Rept. on Contract No. AF 19(604)-8379; April 30, 1962.
- [13] D. A. Johnson, "Microwave Properties of Ceramic Nonlinear Dielectrics," Microwave Lab. Rept. No. 825, Stanford University, Contract No. AF 49(638)-514; July, 1961.
- [14] M. DiDomenico, D. A. Johnson, and R. H. Pantell, "A Ferroelectric Harmonic Generator and the Large Signal Microwave Characteristics of a Ferroelectric Ceramic," Stanford University, Stanford, Calif., Internal Memo. M. L. No. 862; October, 1961.
- [15] M. Cohn, E. S. Cassedy, and M. A. Kott, "TE mode excitation on dielectric loaded parallel plane and trough waveguides," IRE TRANS. ON MICROWAVE THEORY AND TECHNIQUES, vol. MTT-8, pp. 545-552; September, 1960.
- [16] I. E. Balygin and K. S. Porovskii, "Effect of Electrode Metal on Insulation Aging of Ceramic Dielectrics," *Soviet Phys—Tech. Phys.*, vol. 2, p. 459; 1957.
- [17] K. Tomiyasu, "Intrinsic insertion loss of a mismatched microwave network," IRE TRANS. ON MICROWAVE THEORY AND TECHNIQUES, vol. MTT-3, pp. 40-44; January, 1955.
- [18] G. Rupprecht, "Investigation of the Microwave Properties of Ferroelectrics," Research Div., Raytheon Co., Scientific Rept. No. 1, Contract No. AF 19(604)-4085; June, 1960.
- [19] G. Rupprecht, B. D. Silverman, and R. J. Bell, "Investigation of the Microwave Properties of Ferroelectrics," Research Div., Raytheon Co., Final Rept., Contract No. AF 19(604)-4085; October, 1960.

## An Automatic Microwave Phase Comparator\*

J. A. KAISER†, MEMBER, IRE, H. B. SMITH, JR.‡, W. H. PEPPER||, MEMBER, IRE, AND J. H. LITTLE‡

**Summary**—A method for passively measuring the phase angle between two signals of the same frequency is described. While simple in concept, the system has no ambiguities throughout  $360^\circ$  and is independent of relative signal amplitudes because phase angle is displayed orthogonally to amplitude. Consisting principally of two hybrids with detectors and an X-Y indicator, the system contains no moving parts or active phasing devices. In addition to making routine phase measurements, it can be readily applied to automatic direction finders, polarization analyzers, and impedance plotters.

### INTRODUCTION

A SIMPLE method for measuring the relative phase angle between two signals of the same frequency is presented. It differs from previous phase-measuring techniques in that it indicates phase angle automatically and instantaneously without using

modulators<sup>1,2,3</sup> or frequency translators.<sup>4,5</sup> The principle of phase comparison described presents no ambiguities throughout  $360^\circ$  and is independent of relative signal amplitudes.<sup>6</sup> It is classed as a passive system since there are no moving parts or active phasing devices. The measuring speed is limited only by the indicating device.

<sup>1</sup> P. Lacy, "A versatile phase measurement method for transmission line networks," IRE TRANS. ON MICROWAVE THEORY AND TECHNIQUES (*Correspondence*), vol. MTT-9, pp. 568-569; November, 1961.

<sup>2</sup> W. F. Gabriel, "An automatic impedance recorder for X-band," *PROC. IRE*, vol. 42, pp. 1410-1421; September, 1954.

<sup>3</sup> H. A. Dropkin, "Direct reading microwave phase-meter," 1958 IRE NATIONAL CONVENTION RECORD, pt. 1, pp. 57-63.

<sup>4</sup> C. A. Finnila, L. A. Roberts, and C. Susskind, "Measurement of relative phase shift at microwave frequencies," IRE TRANS. ON MICROWAVE THEORY AND TECHNIQUES, vol. MTT-8, pp. 143-147; March, 1960.

<sup>5</sup> R. C. Cumming, "The serrodyne frequency translator," *PROC. IRE*, vol. 45, pp. 175-186; February, 1957.

<sup>6</sup> S. B. Cohn and H. G. Oltman, "A precision microwave phase-measurement system with sweep presentation" 1961 IRE INTERNATIONAL CONVENTION RECORD, New York, N. Y., pt. 3, pp. 147-150. This paper derives detected signals proportional to  $\sin \phi$  and  $\cos \phi$ , as is done here. The ratio of these signals, or  $\tan \phi$ , is displayed on a ratio meter or equivalent to obtain a phase indication which is independent of amplitudes. The possibility of a  $180^\circ$  phase ambiguity does exist, however, when displaying only  $\tan \phi$ .

\* Received June 22, 1962; revised manuscript received August 27, 1962.

† National Aeronautics and Space Administration, Goddard Space Flight Center, Greenbelt, Md. Formerly with Diamond Ordnance Fuze Laboratories.

‡ U. S. Naval Torpedo Station, Keyport, Wash. Formerly with Diamond Ordnance Fuze Laboratories.

|| Diamond Ordnance Fuze Laboratories, Washington, D. C.